The Response of the Ozone Layer to Quadrupled CO2 Concentrations: Implications for Climate

The Response of the Ozone Layer to Quadrupled CO_2 Concentrations: Implications for Climate

GABRIEL CHIODO

Department of Applied Physics and Applied Mathematics, Columbia University, New York, New York, and Institute for Atmospheric and Climate Science, ETH Zürich, Zurich, Switzerland

LORENZO M. POLVANI

Department of Applied Physics and Applied Mathematics, Columbia University, New York, and Lamont-Doherty Observatory, Palisades, and Department of Earth and Environmental Sciences, Columbia University, New York, New York

(Manuscript received 30 January 2019, in final form 19 June 2019)

ABSTRACT

The quantification of the climate impacts exerted by stratospheric ozone changes in abrupt $4 \times CO_2$ forcing experiments is an important step in assessing the role of the ozone layer in the climate system. Here, we build on our previous work on the change of the ozone layer under $4 \times CO_2$ and examine the effects of ozone changes on the climate response to $4 \times CO_2$, using the Whole Atmosphere Community Climate Model. We show that the global-mean radiative perturbation induced by the ozone changes under $4 \times CO_2$ is small, due to nearly total cancellation between high and low latitudes, and between longwave and shortwave fluxes. Consistent with the small global-mean radiative perturbation, the effect of ozone changes on the global-mean surface temperature response to $4 \times CO_2$ is negligible. However, changes in the ozone layer due to $4 \times CO_2$ have a considerable impact on the tropospheric circulation. During boreal winter, we find significant ozone-induced tropospheric circulation responses in both hemispheres. In particular, ozone changes cause an equatorward shift of the North Atlantic jet, cooling over Eurasia, and drying over northern Europe. The ozone signals generally oppose the direct effects of increased CO_2 levels and are robust across the range of ozone changes imposed in this study. Our results demonstrate that stratospheric ozone changes play a considerable role in shaping the atmospheric circulation response to CO_2 forcing in both hemispheres and should be accounted for in climate sensitivity studies.

1. Introduction

Stratospheric ozone, and its response to anthropogenic forcings, provide an important pathway for the coupling between atmospheric composition and climate (Isaksen et al. 2009). Quantifying the impact of that ozone response on tropospheric and surface climate is a key step toward assessing the importance of an interactive stratospheric ozone chemistry in climate change projections and, more generally, on the role of the ozone layer in the climate system.

It has recently been suggested that stratospheric ozone feedbacks can reduce—by up to 20%—the climate sensitivity (Nowack et al. 2015), quantified as the global-mean surface temperature response to abrupt quadrupling of CO_2 (hereafter $4 \times CO_2$). Ozone feedbacks have also been shown to influence the tropospheric circulation response to CO_2, such as a reduction in the poleward shift of the Southern Hemisphere (SH) jet (Chiodo and Polvani 2017), and a strengthening of the Walker circulation (Nowack et al. 2017). However, the magnitude of these feedbacks appears to be model dependent. Most notably, the effect of ozone on climate sensitivity ranges from 20% (Nowack et al. 2015), to 7%–8% (Dietmüller et al. 2014; Muthers et al. 2014), to nil (Marsh et al. 2016). Understanding the origin of this intermodel spread is of crucial importance toward determining whether ozone chemistry feedbacks can significantly contribute to intermodel spread in climate sensitivity.

One possible source of uncertainty in the magnitude of the ozone chemistry feedback is the model dependency of the ozone response to CO_2, and the accompanying (radiative and/or dynamical) effects. As a first step, we examined the response of the ozone layer

Corresponding author: Gabriel Chiodo, chiodo@columbia.edu

DOI: 10.1175/JCLI-D-19-0086.1

to a simple 4 × CO_2 forcing in a recent study (Chiodo et al. 2018, hereafter C18), using four different chemistry–climate models (CCMs). All models showed a decrease in stratospheric ozone concentrations in the tropical lower stratosphere (TLS) (30–100 hPa), and an increase elsewhere in the stratosphere, not unlike the ozone changes seen in future scenarios using anthropogenic greenhouse gases (GHGs) and ozone depleting substances (Zubov et al. 2013; WMO 2014; Douglass et al. 2014). While this pattern is robust, a sizable intermodel spread (up to 40%) was found in the magnitude of the ozone response in the TLS region, which was attributed to spread in tropical upwelling (C18). A similar impact of upwelling on intermodel spread in ozone has also been documented for future CCM projections of ozone recovery (Oman et al. 2010; Douglass et al. 2014). Decreased ozone concentrations in the TLS can induce a substantial radiative perturbation (Hansen et al. 2005) and are thought to be the key element for the strong negative feedback reported by Nowack et al. (2015). There is also uncertainty in the magnitude of the ozone response in high latitudes, although a smaller portion of the spread is explained by dynamical changes there. Overall, spread in lower-stratospheric ozone response can cause uncertainty in the radiative and dynamical response, and hence in the magnitude of the ozone feedbacks.

In addition, even if the model's ozone changes were very similar, different models might have different responses to those changes in ozone, due to differences in their stratospheric zonal wind climatologies (Lin et al. 2017). Both possibilities can be explored, by (i) running one single model using different ozone forcings, or (ii) by running different models with one single ozone forcing. Here, we explore the former.

In this paper, we seek to document the climate implications of changes in the ozone layer under 4 × CO_2, along with their intermodel spread, by specifying the different ozone changes reported in C18 in the same climate model. First, we quantify the radiative forcing exerted by ozone and its changes under 4 × CO_2. Second, we evaluate the ozone-induced temperature and circulation response, by imposing the ozone changes in ocean-coupled model integrations. The forcing (4 × CO_2) and length of the simulations (100 yr) enable us to identify robust responses. Last, specifying ozone as external forcing alongside CO_2 allows us to gather conclusive evidence on the impact of ozone changes on the climate response to increased CO_2 concentrations. These effects are absent in most phase 5 of the Coupled Model Intercomparison Project (CMIP5) simulations, as the vast majority of 4 × CO_2 experiments with those models lack interactive chemistry (Nowack et al. 2018).

2. Models and method

a. Model

In this study we employ the Specified-Chemistry version of the Whole Atmosphere Community Climate Model (SC-WACCM), a stratosphere-resolving version of the National Center for Atmospheric Research (NCAR) Community Earth System Model (CESM), version 1.2.0. The atmospheric model has a resolution of 1.9° longitude by 2° latitude and 66 levels in the vertical domain, with a model top at 5.96 × 10^{-6} hPa (~140 km), and parameterizations for gravity waves. This atmospheric model is coupled to land, ocean and sea ice components, which are identical to those described in Marsh et al. (2013). In SC-WACCM, ozone as well as other chemical species (NO, O, O_2, and CO_2) are prescribed throughout the atmosphere, and not calculated interactively [see Smith et al. (2014) for details]. Hence, SC-WACCM is designed to be run with *prescribed ozone concentrations*, and hence it is ideally suited for this paper's purposes, since it allows us to control the ozone concentrations and investigate their impact on the modeled climate.

In addition to SC-WACCM, we perform offline radiative transfer calculations using the parallel offline radiative transfer, which is part of the Community Earth System Model system (CESM-PORT) (Conley et al. 2013). CESM-PORT uses the same radiative transfer scheme as SC-WACCM, and allows us to calculate the stratosphere-adjusted radiative perturbation induced by ozone, by radiatively equilibrating the temperature profile above the tropopause using the fixed dynamical heating approximation, keeping all tropospheric and surface properties fixed (Conley et al. 2013).

b. Experiments

We start by performing a set of four 100-yr-long ocean-coupled integrations with SC-WACCM using preindustrial control (hereafter referred to as "piControl") forcings for the year 1850 (Table 1) and imposing a fixed (seasonally varying) monthly mean zonal-mean ozone climatology from the four CCMs documented in C18. These are the interactive chemistry version of the CESM model (WACCM; Marsh et al. 2013); the Goddard Institute for Space Studies, version 2, model (GISS-E2-H; Miller et al. 2014); the GFDL Global Coupled Model CM3 (GFDL; Donner et al. 2011); and the coupled model for studies of Solar-Climate-Ozone Links (SOCOL; Stenke et al. 2013).

By running SC-WACCM piControl integrations with an ozone forcing derived from each of these CCMs, we test the impact of differences in the ozone climatology across these models (cf. C18, their Fig. S2) on the mean climate of SC-WACCM. We find that imposing the

TABLE 1. List of SC-WACCM integrations analyzed in this study. All experiments are performed with coupled land, ocean, and sea ice components, and are 100 yr long.

Expt	CO_2 (ppmv)	O_3 forcing	
WPI	287	piControl	WACCM O_3
W4x	1148	piControl	
$W4xO_3$	1148	$4 \times CO_2$	
GPI	287	piControl	GFDL O_3
G4x	1148	piControl	
$G4xO_3$	1148	$4 \times CO_2$	
SPI	287	piControl	SOCOL O_3
S4x	1148	piControl	
$S4xO_3$	1148	$4 \times CO_2$	

piControl ozone from WACCM, GFDL, and SOCOL has a negligible effect on the zonal-mean temperature and wind climatology simulated by SC-WACCM. On the other hand, imposing the ozone climatology from GISS-E2-H into SC-WACCM leads to a significantly warmer polar stratosphere (by 5 K), a much weaker stratospheric polar vortex (by 6 m s^{-1}) and an increase in the frequency of sudden stratospheric warmings (SSWs) in SC-WACCM from 0.4 SSWs yr^{-1} (Smith et al. 2014) to 0.7 SSWs yr^{-1}. This is due to much larger polar cap ozone abundances in GISS-E2-H compared to other CCMs (cf. C18, their Fig. S2), and the resulting enhanced SW absorption resulting from imposing this ozone climatology in SC-WACCM (not shown). Because of this bias in the circulation, we have decided to discard the ozone forcing from GISS-E2-H and use only the ozone datasets from three models in this study: WACCM, GFDL, and SOCOL. An additional reason behind this choice is that by keeping the ozone forcings that do not significantly alter the basic state in SC-WACCM, we obtain a common "reference state" to which the climate change impacts from $4 \times CO_2$ can be compared to.

Then, for each of these three ozone datasets, we perform two additional runs with SC-WACCM: an abrupt $4 \times CO_2$ using a preindustrial ozone climatology ("4x" suffix in Table 1), and an abrupt $4 \times CO_2$ using $4 \times CO_2$ ozone ("$4xO_3$" suffix in Table 1). This yields a total of nine 100-yr SC-WACCM runs: three using the ozone from the WACCM model (WPI, W4x, and $W4xO_3$), three using the ozone from the GFDL model (GPI, G4x, and $G4xO_3$) and three using the ozone from the SOCOL model (SPI, S4x, and $S4xO_3$; see Table 1). Each of the three ozone forcing datasets was obtained from the climate sensitivity runs (i.e., piControl and $4 \times CO_2$) of the corresponding CCMs, and we have already documented those ozone datasets in C18. We prescribe a seasonally varying monthly mean zonal-mean (2D) ozone climatology derived from the three CCMs, and linearly interpolate that ozone field onto the vertical and horizontal grid of SC-WACCM. In all cases, we keep the ozone depleting substances (ODS), and all forcings except CO_2 fixed at 1850 levels. Given the lack of ozone-hole formation in these runs, prescribing monthly mean zonal-mean ozone is unlikely to introduce the biases documented in modeling studies that have focused on ozone depletion (Neely et al. 2014; Seviour et al. 2016).

Accordingly, the ozone changes with the $4 \times CO_2$ forcing in one set of perturbed integrations ($4xO_3$), but not in the other (4x). The difference between 4x and PI runs quantifies the climate response to CO_2 in the absence of any ozone changes in SC-WACCM (i.e., W4x minus WPI for WACCM, G4x minus GPI for GFDL, and S4x minus SPI for SOCOL). In contrast, the difference between $4xO_3$ and 4x quantifies the impact of ozone changes resulting from $4 \times CO_2$ on the climate system: this is the key aim of the present paper.

To quantify the radiative perturbation arising from ozone changes, we perform offline calculations using CESM-PORT, imposing the ozone changes under $4 \times CO_2$. For each of the three ozone climatologies (WACCM, GFDL, and SOCOL), we compute a reference case with a piControl ozone climatology. Then, we add the ozone response to $4 \times CO_2$, derived from each of the three models. Each of the CESM-PORT runs is 5 years long, allowing the stratosphere to reach radiative equilibrium. Finally, we take differences in the radiative flux at the piControl tropopause between each perturbed and reference case, to obtain the stratosphere-adjusted radiative flux change induced by the ozone response to $4 \times CO_2$ in each of the CCMs; we will refer to these as R_{adj}.

c. *The imposed ozone forcing*

We first present the annual-mean ozone response to $4 \times CO_2$ simulated by three coupled CCMs: WACCM, GFDL, and SOCOL. More specifically, we analyze the ozone response in the runs using interactive chemistry from these CCMs; this response is used to prescribe ozone in the SC-WACCM and PORT runs. Following C18, the ozone response is quantified as the difference between the piControl and the last 50 years of the $4 \times CO_2$ runs of each of the CCMs, and is shown in number density units in Fig. 1 for WACCM (Fig. 1a), GFDL (Fig. 1b), and SOCOL (Fig. 1c). For simplicity, we will refer to these ozone changes as $\Delta O_3(4 \times CO_2)$ throughout the paper. As reported in C18, the pattern of $\Delta O_3(4 \times CO_2)$ at low latitudes consists of an increase in the upper stratosphere (1–10 hPa) ozone, a decrease in the TLS ozone, and negligible changes in tropospheric ozone (Fig. 1). The upper-stratospheric ozone increase is linked to the CO_2-induced radiative cooling, which

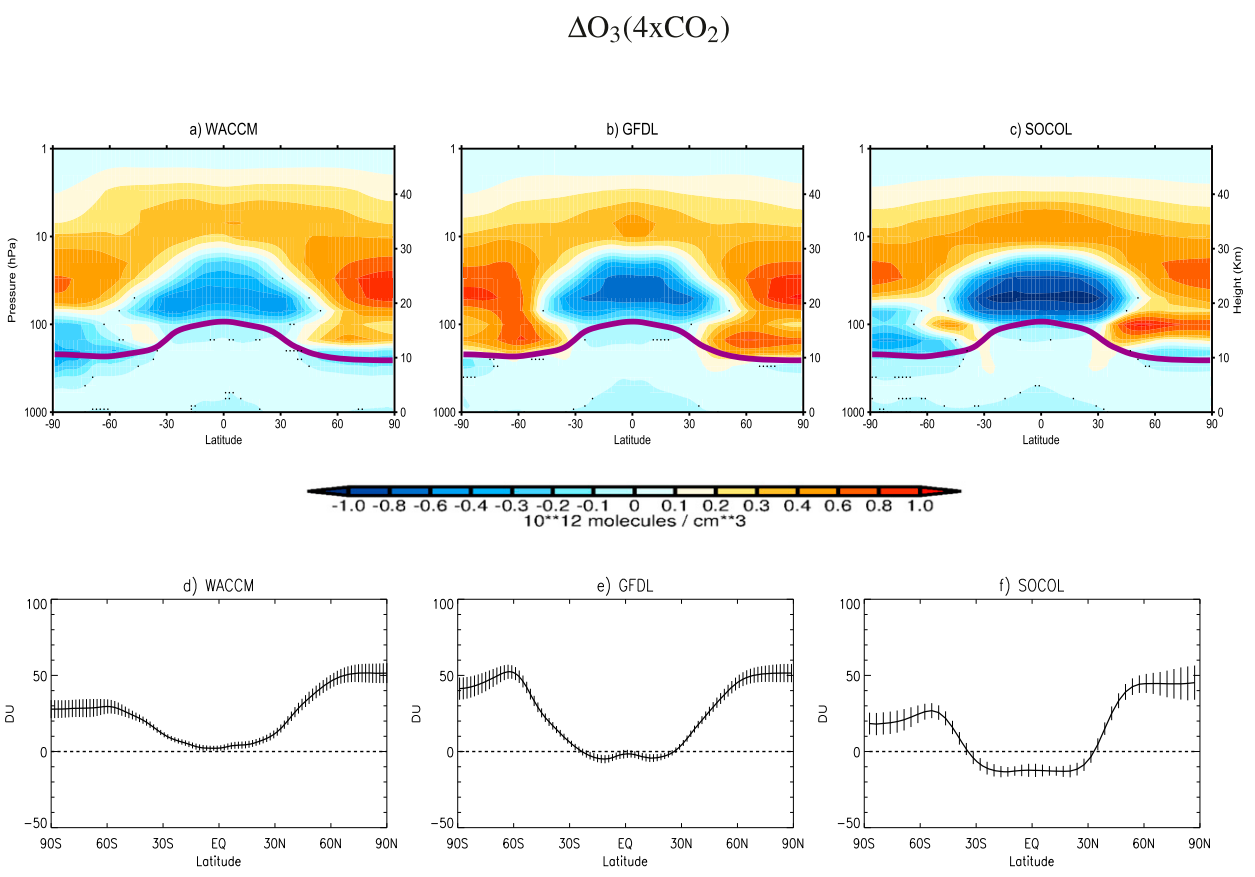

FIG. 1. Annual-mean zonal-mean ozone response to $4 \times CO_2$ [$\Delta O_3(4 \times CO_2)$] in number density units (molecules cm^{-3}) for the coupled runs from (a) WACCM, (b) GFDL, and (c) SOCOL. The thick violet line identifies the thermal tropopause for the piControl experiment. Nonsignificant differences (at the 95% confidence level) are stippled. Annual-mean zonal-mean response in the stratospheric ozone column in (d) WACCM, (e) GFDL, and (f) SOCOL model. Units: Dobson units (DU).

affects the reaction rates involved in the Chapman cycle, resulting in increased ozone concentrations (Haigh and Pyle 1982; Jonsson et al. 2004). On the other hand, the TLS ozone decrease is linked to enhanced tropical upwelling (Shepherd 2008). At high latitudes and in both hemispheres, ozone increases in the stratosphere (10–100 hPa), with larger increases in the NH. Calculating $\Delta O_3(4 \times CO_2)$ in number density units rather than mixing ratio (cf. C18, their Fig. S1) allows us to more directly relate ozone changes with radiative absorption changes (Goody and Yung 1989), highlighting stratospheric regions where ozone changes mostly contribute to R_{adj}, and hence its possible climate effects.

As reported in C18, while the pattern of $\Delta O_3(4 \times CO_2)$ is quite similar among the models, there are differences in the magnitude. For example, SOCOL shows much larger TLS ozone decrease (Fig. 1c), a feature linked to larger tropospheric warming and upwelling from $4 \times CO_2$ in that model (C18). Conversely, the GFDL model shows a larger ozone increase in the extratropical lower stratosphere than the other two models (Fig. 1b). As a result of this uncertainty, the stratospheric column ozone (SCO) response in the tropics is uncertain, as some models show weakly positive SCO increases (WACCM) while others (GFDL and SOCOL) show decreases (Figs. 1d,e). Note that a very similar pattern is obtained when using the full (150 yr) difference rather than just the last 50-yr portion of the $4 \times CO_2$ runs, as ozone quickly equilibrates within the first few decades of the $4 \times CO_2$ runs.

3. Impact of ozone forcing on radiative fluxes and climate sensitivity

Next, we evaluate the influence of the ozone changes under $4 \times CO_2$ discussed in the previous section, by imposing them in one single model (SC-WACCM), and by analyzing the resulting climate change. We start by computing the annual-mean zonal-mean R_{adj} resulting from $\Delta O_3(4 \times CO_2)$ derived from each of the three CCMs: this is plotted in Fig. 2 for the shortwave (SW, blue), longwave (LW, red), and net (black) components. Recall that the ozone layer strongly absorbs solar

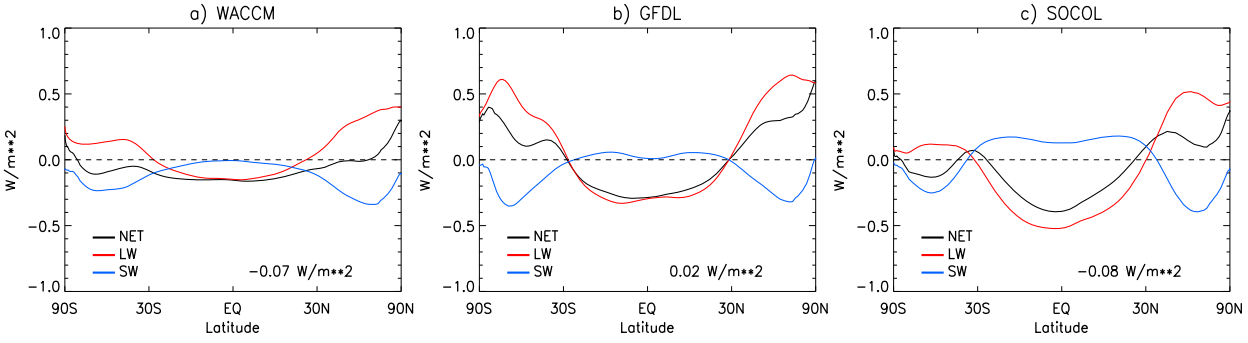

FIG. 2. Annual-mean zonal-mean stratosphere-adjusted radiative flux change at the tropopause (R_{adj}) induced by $\Delta O_3(4 \times CO_2)$ in (a) WACCM, (b) GFDL, and (c) SOCOL. The red and blue lines show the LW and SW (R_{adj}), respectively, while the black line identifies the net forcing. Numbers indicate the global area-weighted mean $\langle R_{adj} \rangle$. Units: W m^{-2}.

radiation, resulting in a reduction of the incident SW flux at the tropopause (Ramanathan and Dickinson 1979; Lacis et al. 1990). Hence, changes in SCO under $4 \times CO_2$ (Figs. 1d,f) will either reinforce or weaken the radiative effect of the piControl ozone, thereby determining the sign of the SW R_{adj} (blue line in Fig. 2). In response to $4 \times CO_2$, SCO increases in the polar regions (Figs. 1d,f); this reduces the incident SW flux, leading to a negative SW R_{adj}. In the tropics, SCO changes in the three CCMs are small (Figs. 1d,f), resulting in a small SW R_{adj}.

Conversely, the LW R_{adj} (red line in Fig. 2) is largely influenced by *local* perturbations in ozone abundances near the tropopause, as these affect the absorption of LW and SW radiation, leading to temperature changes, and consequently in LW emission (Ramanathan and Dickinson 1979; Lacis et al. 1990). As the largest ozone number density changes are found in the lower stratosphere (Fig. 1), it is the ozone response in this region that largely determines the LW R_{adj}. Ozone decreases in the TLS reduce SW absorption, leading to cooling and consequently a negative LW R_{adj}. Conversely, lower-stratospheric ozone increases in the mid- and high latitudes exert a positive LW R_{adj}.

Although the LW and SW flux changes are opposite in sign, the net R_{adj} can be locally as large as 0.5 W m^{-2}. Most importantly, the net R_{adj} (black line in Fig. 2) is negative in the tropics, and positive at high latitudes. As a result of oppositely signed R_{adj} in high and low latitudes, $\langle R_{adj} \rangle$ (where $\langle\ \rangle$ denote area-weighted global mean) is small: -0.07, 0.02, and -0.08 W m^{-2}. This cancellation is robust in all three ozone datasets, indicating a small radiative perturbation from $\Delta O_3(4 \times CO_2)$. Replacing the piControl with the $4 \times CO_2$ tropopause in the offline PORT calculations has a small impact on the results (i.e., 5%–10%). Hence, the R_{adj} values shown in Fig. 2 are robust to the tropopause definition.

It has been suggested that most of the climate impacts of ozone changes under $4 \times CO_2$ forcing originates from the ozone decrease in the TLS region (Nowack et al. 2015), owing to the large radiative efficiency of perturbations in the cold-trap region (Hansen et al. 2005). We confirm this feature here across all three ozone datasets; it is largest in SOCOL, consistent with the larger TLS decrease in that ozone (Fig. 1c). However, ozone in the extratropical lower stratosphere (30°–50°N) increases in all models, including SOCOL, leading to positive LW R_{adj} there, which counteracts the negative LW R_{adj} in the tropics. As a result, the radiative perturbation from $\Delta O_3(4 \times CO_2)$ is negligible, even in ozone datasets exhibiting larger changes in the lower stratosphere, such as SOCOL.

While R_{adj} gives an indication of the potential effects on global-mean surface temperature $\langle T_s \rangle$ (Myhre et al. 2013), it need not be a good predictor of the $\langle T_s \rangle$ equilibrium response, especially in the case of spatially and vertically nonhomogeneous forcing agents, such as ozone (see, e.g., Joshi et al. 2003; Stuber et al. 2005). To quantify the effects of ozone on climate sensitivity, simulations with coupled ocean are needed.

So, we now turn to the ocean-coupled SC-WACCM integrations, to establish if ozone changes due to $4 \times CO_2$ alter the climate sensitivity. The $\langle T_s \rangle$ evolution for the three sets of SC-WACCM integrations listed in Table 1 is shown in Fig. 3. Here, we show the piControl integrations (dash–dotted), the $4 \times CO_2$ integrations with piControl ozone (dotted lines) and the $4 \times CO_2$ integrations with ozone from $4 \times CO_2$ (bold lines): the three colors indicate WACCM ozone (blue), GFDL ozone (green), and SOCOL ozone (red). We see that the piControl integrations (WPI, GPI, and SPI) are virtually identical. More importantly, the temperature increase simulated after 100 years is identical, whether one uses piControl ozone or $4 \times CO_2$ ozone (Fig. 3). This same result is also seen in individual seasons (e.g., DJF and JJA, not shown), and suggests

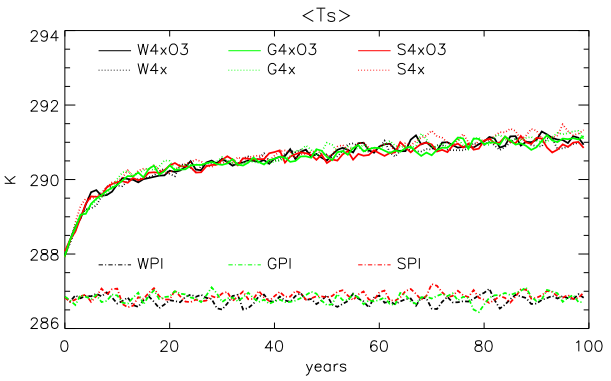

FIG. 3. Time series of global area-weighted mean surface temperature $\langle T_s \rangle$ in the nine SC-WACCM model integrations listed in Table 1. The dash–dotted lines identify the piControl integrations, specifying the piControl ozone climatology obtained from the WACCM (WPI), GFDL (GPI), and SOCOL (SPI) model runs documented in C18. The dotted and thick lines identify the $4 \times CO_2$ integrations using SC-WACCM, specifying the piControl and $4 \times CO_2$ ozone climatology, respectively, obtained from WACCM (W4x and W4xO_3), GFDL (G4x and G4xO_3), and SOCOL (S4x and S4xO_3). Units: K.

that the ozone forcing does not alter the climate sensitivity in SC-WACCM, consistent with the small $\langle R_{adj} \rangle$ shown in Fig. 2. From this, we can conclude that model-dependencies in the ozone feedback seen in earlier studies (Dietmüller et al. 2014; Muthers et al. 2014; Nowack et al. 2015; Marsh et al. 2016) are likely to be due to differences in the models, and not due to differences in $\Delta O_3(4 \times CO_2)$.

According to these results, any feedbacks resulting from $\Delta O_3(4 \times CO_2)$ do not affect the global-mean surface temperature of our model, confirming previous findings (Marsh et al. 2016), and expanding on them, as these results hold for two additional ozone datasets showing larger ozone changes in the TLS (and consequently larger negative R_{adj}), notably SOCOL. Climate sensitivity, quantified in terms of global-mean surface temperature response to CO_2, is an important metric for model intercomparisons, as it captures many aspects of a climate model's response to CO_2 forcing (Knutti and Hegerl 2008; Knutti et al. 2017). However, the atmospheric circulation response exerts a larger control on regional aspects of climate change than global-mean surface temperature (Grise and Polvani 2014a; Shepherd 2014). Hence, we next evaluate the impact of $\Delta O_3(4 \times CO_2)$ on the modeled atmospheric circulation response to $4 \times CO_2$ in SC-WACCM, in other words the impact of ozone changes on the "dynamical sensitivity" (Grise and Polvani 2014a). It has been shown that dynamical sensitivity correlates poorly with climate sensitivity in the midlatitudes (Grise and Polvani 2016).

4. Impact of ozone forcing on the atmospheric circulation response to CO_2

a. *Temperature*

We start by examining the annual-mean zonal-mean temperature response from SC-WACCM in Fig. 4. In the top row, we plot the response to $4 \times CO_2$ alone with ozone fixed at piControl levels (Figs. 4a–c). As expected, the $4 \times CO_2$ responses in SC-WACCM exhibit the characteristic pattern of tropospheric warming and stratospheric cooling; this is nearly identical in the three runs, even though these use different piControl ozone climatologies (Figs. 4a–c), suggesting that the structure of the temperature response to $4 \times CO_2$ in SC-WACCM is largely insensitive to intermodel differences in the piControl ozone climatology.

Next, we quantify the influence of $\Delta O_3(4 \times CO_2)$ on the response in SC-WACCM, by differencing the three sets of $4 \times CO_2$ integrations, using $4 \times CO_2$ (W4xO_3, G4xO_3, S4xO_3) versus piControl ozone (W4x, G4x, S4x), as shown in Figs. 4d–f. It is clear that $\Delta O_3(4 \times CO_2)$ induces cooling in the TLS and warming elsewhere in the stratosphere (Figs. 4d–f). In the tropics, the structure is coherent with the pattern of $\Delta O_3(4 \times CO_2)$ (Fig. 1). The ozone-induced TLS cooling ranges between 2 and 4 K in the runs using WACCM and SOCOL ozone forcings, respectively (Figs. 4d–f), consistent with the spread across these datasets in the magnitude of ozone decrease in that region (Fig. 1). This indicates that the ozone-induced TLS cooling is largely a result of reduced SW absorption. At high latitudes on the other hand, the spread in the lower-stratospheric warming is not as strongly correlated with the spread in ozone forcing, suggesting that dynamical heating (which is less linearly related to ozone abundancies than SW absorption) plays a larger role.

Via its effects on TLS temperature, $\Delta O_3(4 \times CO_2)$ also causes a reduction in stratospheric water vapor concentrations in SC-WACCM (not shown); this ranges between 10% in the runs using WACCM ozone, 15% in those using GFDL ozone, and 25% in those using SOCOL ozone. Hence, changes in the stratospheric water vapor feedback induced by ozone (Stuber et al. 2001, 2005; Dietmüller et al. 2014; Nowack et al. 2015) are captured in our SC-WACCM runs, but their effects on tropospheric and surface climate are negligible. The key result here is that in the lower stratosphere, the temperature response to $\Delta O_3(4 \times CO_2)$ (Figs. 4d–f) is of same order of magnitude as the response to CO_2 in this region (Figs. 4a–c), indicating that ozone can substantially alter the CO_2-induced stratospheric cooling. This is consistent with the impact of ozone forcing in RCP scenarios documented in Maycock (2016). In the

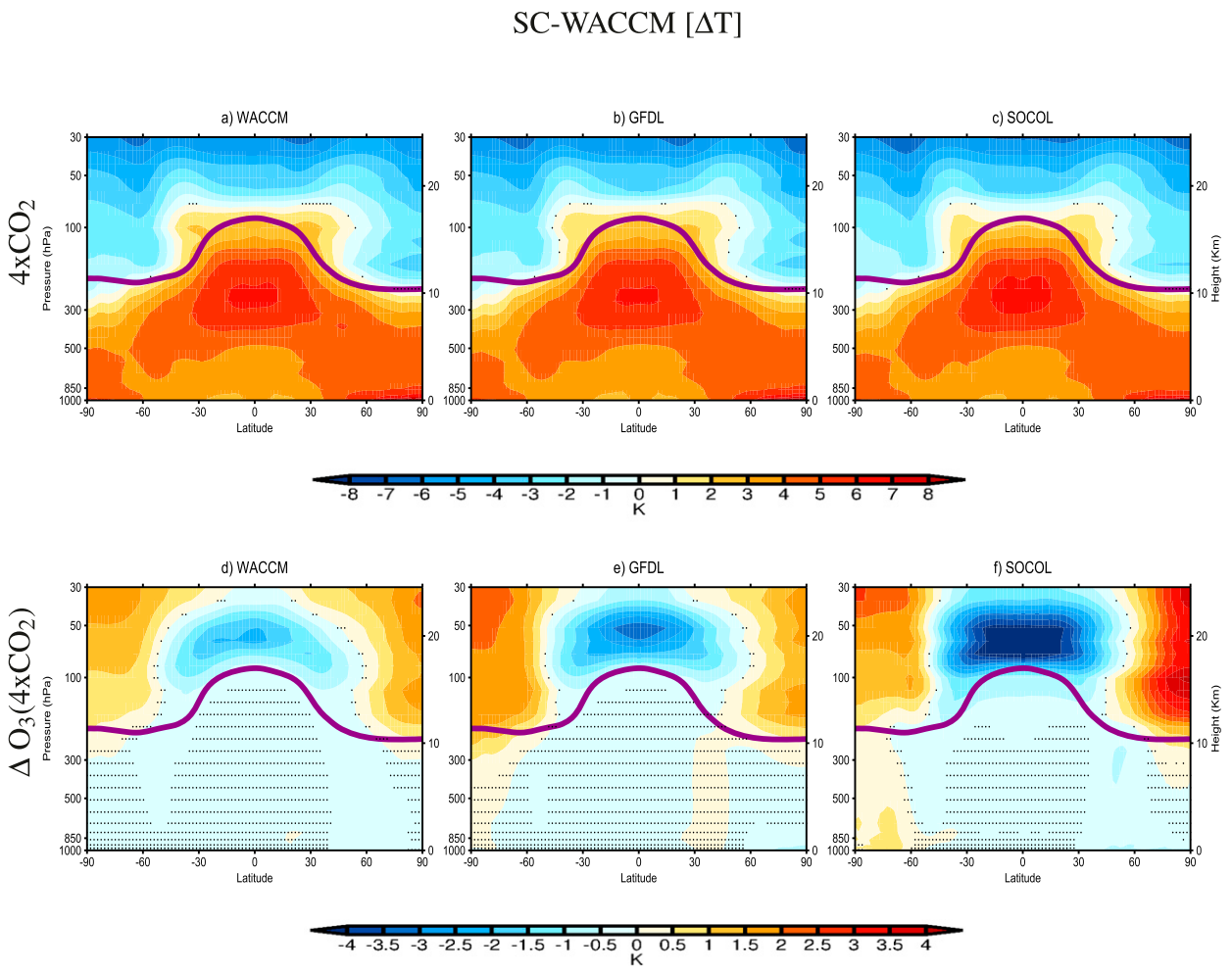

FIG. 4. (a)–(c) Annual-mean zonal-mean temperature response to $4 \times CO_2$, in SC-WACCM integrations imposing the piControl ozone climatology from (a) WACCM (W4x-WPI), (b) GFDL (G4x-GPI), and (c) SOCOL (S4x-SPI). (d)–(f) Change in zonal-mean temperature in SC-WACCM, induced by $\Delta O_3(4 \times CO_2)$ in (d) WACCM ($W4xO_3$-W4x), (e) GFDL ($G4xO_3$-G4x), and (f) SOCOL ($S4xO_3$-S4x). Nonsignificant differences (at the 95% confidence level) are stippled. Units: K.

stratosphere (30–70 hPa), the pattern of temperature change due to $\Delta O_3(4 \times CO_2)$ changes sign between tropics and high latitudes, while the temperature response to $4 \times CO_2$ monotonically increases with height, with little variation across different latitudes. CO_2 induces a change in the meridional temperature gradient, but only in the lowermost extratropical stratosphere (100–300 hPa).

b. Zonal wind

The temperature response to $\Delta O_3(4 \times CO_2)$ implies a reduction in the meridional temperature gradient near the tropopause, which has major consequences for the atmospheric circulation in SC-WACCM, as shown next. The annual-mean zonal-mean zonal wind response to $4 \times CO_2$ in the absence of ozone change (W4x, G4x, S4x) is plotted in Figs. 5a–c. In response to $4 \times CO_2$, we see the well-known strengthening of the westerlies in the stratosphere, and the poleward migration of the tropospheric midlatitude jet in both hemispheres, as indicated by the dipole of positive (negative) anomalies of 0.5–1 m s^{-1} poleward (equatorward) of the climatological location of the wind maximum at 850–500 hPa (Figs. 5a–c). This feature is seen in both hemispheres, although the largest signal is in the SH, consistent with the CMIP5 models (Barnes and Polvani 2013; Grise and Polvani 2014b).

Let us now consider the impact of ozone changes from $4 \times CO_2$, shown in Figs. 5d–f, starting from the SH. An important result of our study is that $\Delta O_3(4 \times CO_2)$ leads to zonal-mean zonal wind anomalies of opposite sign in the stratosphere (i.e., easterlies), which extend to the troposphere in the SH in the annual mean (Figs. 5d–f).

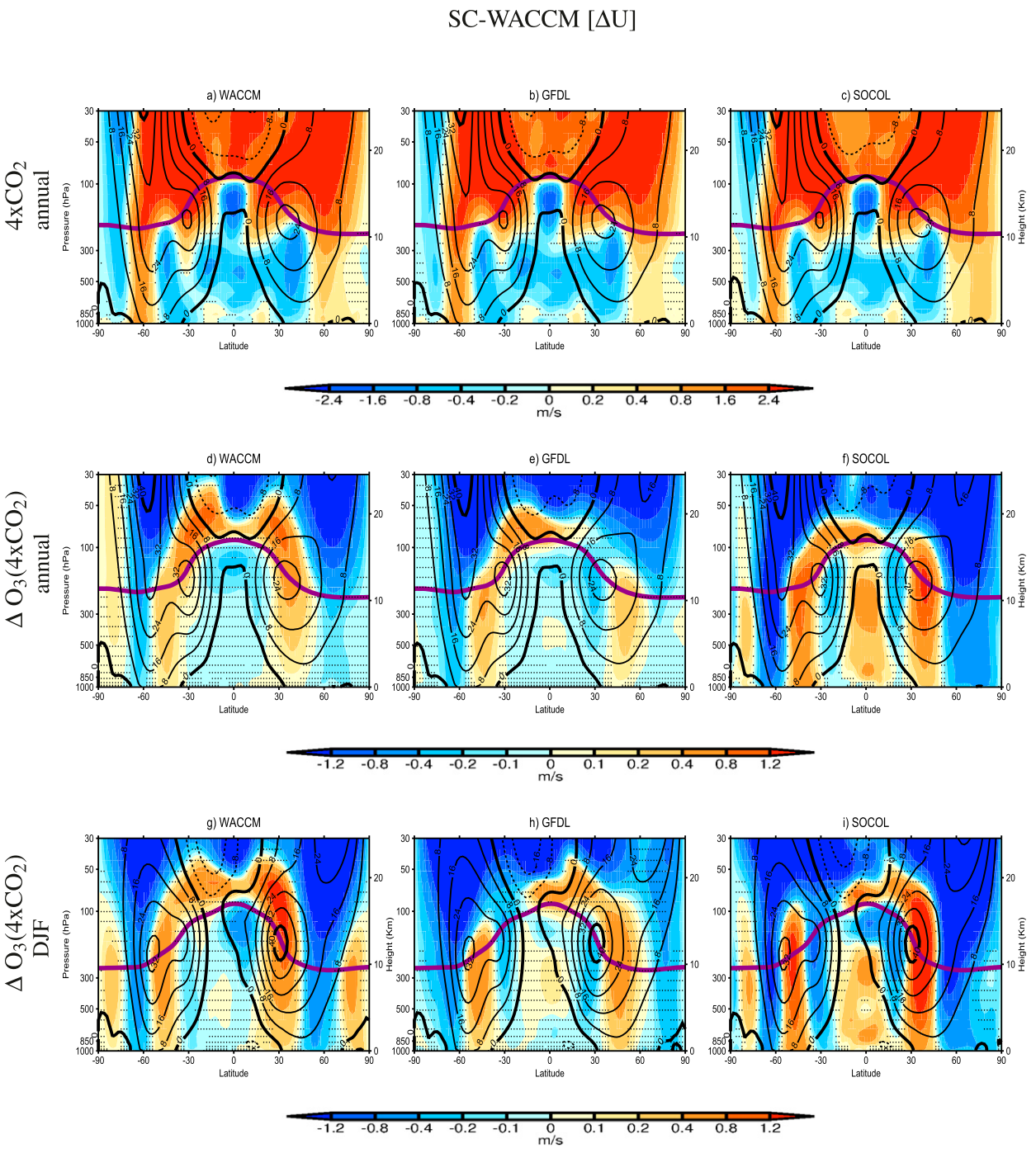

FIG. 5. As in Fig. 4, but for annual-mean zonal-mean zonal wind from the SC-WACCM runs. Black contour lines show climatological zonal-mean zonal wind in each SC-WACCM piControl experiment using piControl ozone climatologies [i.e., (a),(d) WPI for WACCM, (b),(e) GPI for GFDL, and (c),(f) SPI for SOCOL]. (g)–(i) Boreal winter (DJF) mean response to $\Delta O_3(CO_2)$ simulated by SC-WACCM (panels). Units: m s^{-1}. Nonsignificant differences (at the 95% confidence level) are stippled.

This SH signal is largest during DJF (Figs. 5g–i), suggesting a reduction of the austral circulation response to CO_2 in that season, as reported in Chiodo and Polvani (2017). This SH effect is robust across different ozone datasets, although the magnitude depends on the specific ozone dataset, being largest for SOCOL ozone (Fig. 5i) and smallest for the WACCM ozone (Fig. 5g). In the annual mean, SC-WACCM integrations with piControl

TABLE 2. $4 \times CO_2$ response in latitudinal position of the midlatitude jet in SC-WACCM, calculated based on 850 hPa zonal-mean zonal wind, for (first column) SH annual mean, (second column) SH in DJF, (third column) North Atlantic (0°–90°N, 60°W–0°) in DJF, and (fourth column) North Pacific (0°–90°N, 135°E–125°W) in DJF. Negative (positive) numbers mean southward (northward) shift in degrees latitude; confidence intervals indicate the standard deviation of the mean.

Difference	SH ANN (°)	SH DJF (°)	North Atlantic DJF (°)	North Pacific DJF (°)
W4x–WPI	−0.9 ± 0.1	−1.6 ± 0.1	+1.7 ± 0.3	+3.1 ± 0.4
W4xO_3–WPI	−0.7 ± 0.1	−1.3 ± 0.1	+0.8 ± 0.3	+2.3 ± 0.3
G4x–GPI	−1.1 ± 0.1	−1.8 ± 0.1	+1.9 ± 0.3	+3.1 ± 0.4
G4xO_3–GPI	−0.8 ± 0.1	−1.4 ± 0.1	+0.7 ± 0.3	+3.5 ± 0.3
S4x–SPI	−1.1 ± 0.1	−1.8 ± 0.1	+1.4 ± 0.4	+2.6 ± 0.3
S4xO_3–SPI	−0.4 ± 0.1	−1.2 ± 0.1	+0.1 ± 0.3	+2.0 ± 0.2

ozone climatology under $4 \times CO_2$ exhibit a southward (i.e., poleward) shift in the SH jet location (calculated based on zonal-mean zonal wind at 850 hPa) of 0.9°–1.1° (Table 2). When ozone changes are included, a smaller shift (by 20%–50%) is found (Table 2).

More importantly, in DJF, even in the NH ozone changes cause a significant change in zonal-mean zonal wind in SC-WACCM (Figs. 5g–i). The seasonality of the NH tropospheric circulation response is consistent with the seasonality of Arctic ozone, whose increase in response to $4 \times CO_2$ in the coupled CCMs peaks around boreal winter and spring (cf. C18, their Fig. 8). Jet shifts in the SH are well known to be caused by ODS-induced ozone changes (WMO 2014). Unlike the case of ODS-induced ozone depletion, we find here that ozone changes induced by CO_2 are capable of shifting the midlatitude jet even in the NH: this is a key result of this paper.

Unlike the SH, the tropospheric circulation in the NH is less zonally symmetric. Hence, zonal averaging may mask zonally asymmetric features (e.g., Barnes and Polvani 2013; Grise and Polvani 2014b). Thus, we analyze next the near-surface (850 hPa) zonal wind response to CO_2 during boreal winter in SC-WACCM (Fig. 6). First, we see that $4 \times CO_2$ leads to positive (negative) zonal wind anomalies on the poleward (equatorward) flank of the Pacific jet located at 40°N and in the Atlantic basin near 50°N (Figs. 6a–c). Most importantly, $\Delta O_3(4 \times CO_2)$ leads to the opposite pattern (Figs. 6d–f), consisting of negative (positive) anomalies on the poleward (equatorward) side of the midlatitude jets. Over the North Atlantic, this pattern is robust across all three ozone forcings, and is associated with positive sea level pressure (SLP) anomalies over the Arctic, which are reminiscent of a negative North Atlantic Oscillation (NAO) pattern (not shown).

Contrasting the jet latitude in the model runs, we find a poleward shift of the North Atlantic jet in response to $4 \times CO_2$ of 1.4°–1.9° without ozone changes (see Table 2). The SC-WACCM integrations using the ozone forcing from $4 \times CO_2$ simulate a much smaller poleward shift, ranging between 0.8° (WACCM ozone forcing) and 0.1° (SOCOL ozone forcing). Hence, $\Delta O_3(4 \times CO_2)$ substantially reduces the poleward shift of the Atlantic jet due to CO_2 in SC-WACCM, with the reduction ranging between ~50% (WACCM ozone forcing) and a near-*complete* cancellation (SOCOL ozone forcing). Over the North Pacific, a similar reduction is seen, with the exception of the runs forced with GFDL ozone (Table 2). These results are consistent with the ozone-induced temperature perturbation near the tropopause, and the resulting change in the meridional temperature gradient at these levels, being largest in the S4xO_3 run (Fig. 4f) due to larger TLS ozone decrease in the SOCOL model (Fig. 1c).

c. *Surface temperature and precipitation patterns*

Are these changes in the NH tropospheric circulation also associated with changes in regional climate? To answer this question, we turn to the DJF surface temperature response to CO_2 and $\Delta O_3(4 \times CO_2)$, which is plotted in Fig. 7. In the absence of ozone changes, the $4 \times CO_2$ forcing leads to warming of up to 8 K over the Arctic, northern Eurasia, and North America (Figs. 7a–c). Interestingly, $\Delta O_3(4 \times CO_2)$ leads to cooling over wide parts of Eurasia (Figs. 7d–f) up to 1.6 K in the SOCOL ozone run, that is, a 20% reduction of the warming due to $4 \times CO_2$. This local temperature change is consistent with the southward shift of the North Atlantic jet induced by $\Delta O_3(4 \times CO_2)$ shown in Figs. 6d–f, resulting in reduced heat advection in Eurasia (Hurrell et al. 2003). A similar pattern is also typically observed in the aftermath of sudden stratospheric warmings (Baldwin and Dunkerton 2001; Charlton and Polvani 2007), consistent with easterly wind anomalies in the NH polar stratosphere (Figs. 5g–i).

Changes in the near-surface zonal wind over the North Atlantic are typically associated with changes in precipitation: these are plotted in Fig. 8. In response to CO_2 alone, we find drying over the subtropical Atlantic and Mediterranean basin, and wetting northward of 45°N (Figs. 8a–c); this is in agreement with CMIP5 model projections in high emission scenarios (cf. Collins et al. 2013, their Fig. 12.22). Again, $\Delta O_3(4 \times CO_2)$ leads

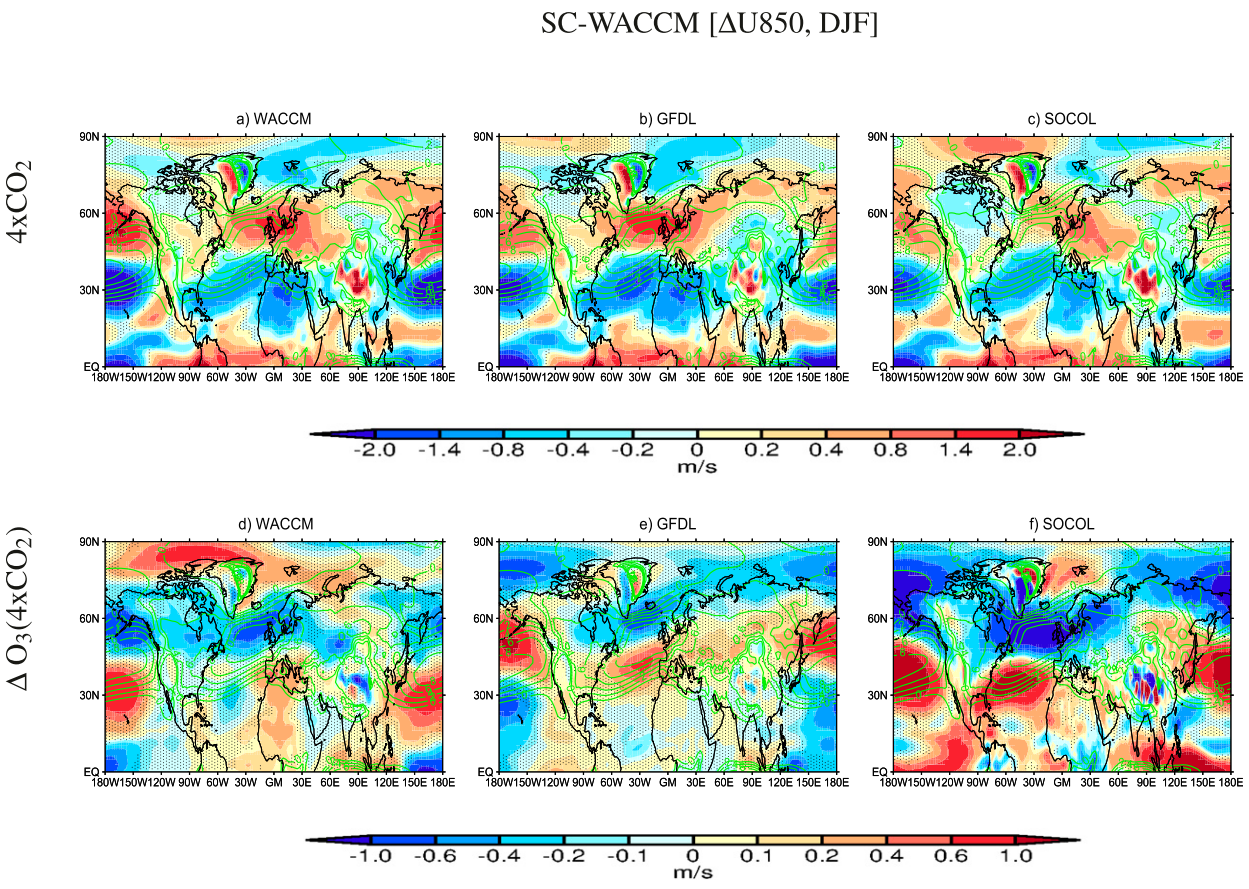

FIG. 6. (a)–(c) Boreal winter (DJF) mean response to $4 \times CO_2$ in zonal wind at 850 hPa in SC-WACCM integrations imposing piControl ozone climatology from the (a) WACCM, (b) GFDL, and (c) SOCOL model. (d)–(f) Change in zonal wind at 850 hPa in SC-WACCM, induced by $\Delta O_3(4 \times CO_2)$ in the (d) WACCM, (e) GFDL, and (f) SOCOL model. Green contour lines show the climatological zonal wind in each piControl experiment. Units: m s^{-1}. Nonsignificant differences (at the 95% confidence level) are stippled.

to the opposite pattern: drying over the northern portion of the North Atlantic and parts of Scandinavia, and wetting over central/southern Europe, although the location and magnitude of the peak anomalies varies among the experiments. The precipitation changes can be locally as large as 0.4–0.6 mm day^{-1}, which constitutes a large fraction (~40%) of the local precipitation response to $4 \times CO_2$. Overall, these signals are consistent with surface climate responses to Arctic ozone variability reported in earlier studies (Smith and Polvani 2014; Calvo et al. 2015; Ivy et al. 2017).

These results suggest that the ozone layer, via its response to $4 \times CO_2$, can significantly alter the tropospheric circulation in both hemispheres. In a nutshell, increases in CO_2 concentrations cause an acceleration of the Brewer–Dobson circulation, as well as stratospheric cooling. In the lower stratosphere, these result in a decrease in ozone abundances in the tropics and an increase in the high latitudes. These ozone responses lead to a reduction of the meridional temperature gradient near the tropopause on both sides of the equator, which weakens the stratospheric polar vortex. In the NH, this is in turn associated with surface signals over the Atlantic basin, such as a southward displacement of the Atlantic jet, cooling over Eurasia, and drying over portions of northern Europe. Hence, changes in the ozone layer due to $4 \times CO_2$ prove to be a strong mitigating factor to increasing CO_2.

Presently, plans for CMIP6 indicate that models that do not interactively simulate ozone chemistry (i.e., the vast majority) will run $4 \times CO_2$ experiments using prescribed preindustrial ozone concentrations (Eyring et al. 2016), and may thus neglect the effects documented in this paper. It is also worth noting that the stratospheric ozone changes under $4 \times CO_2$ documented in this paper are similar in magnitude to those occurring in 2080–2100 under the RCP8.5 scenario, due to concomitant influence of decreasing ODS emissions in the latter (not shown). Hence, the changes in surface climate documented in this paper are highly relevant to more realistic

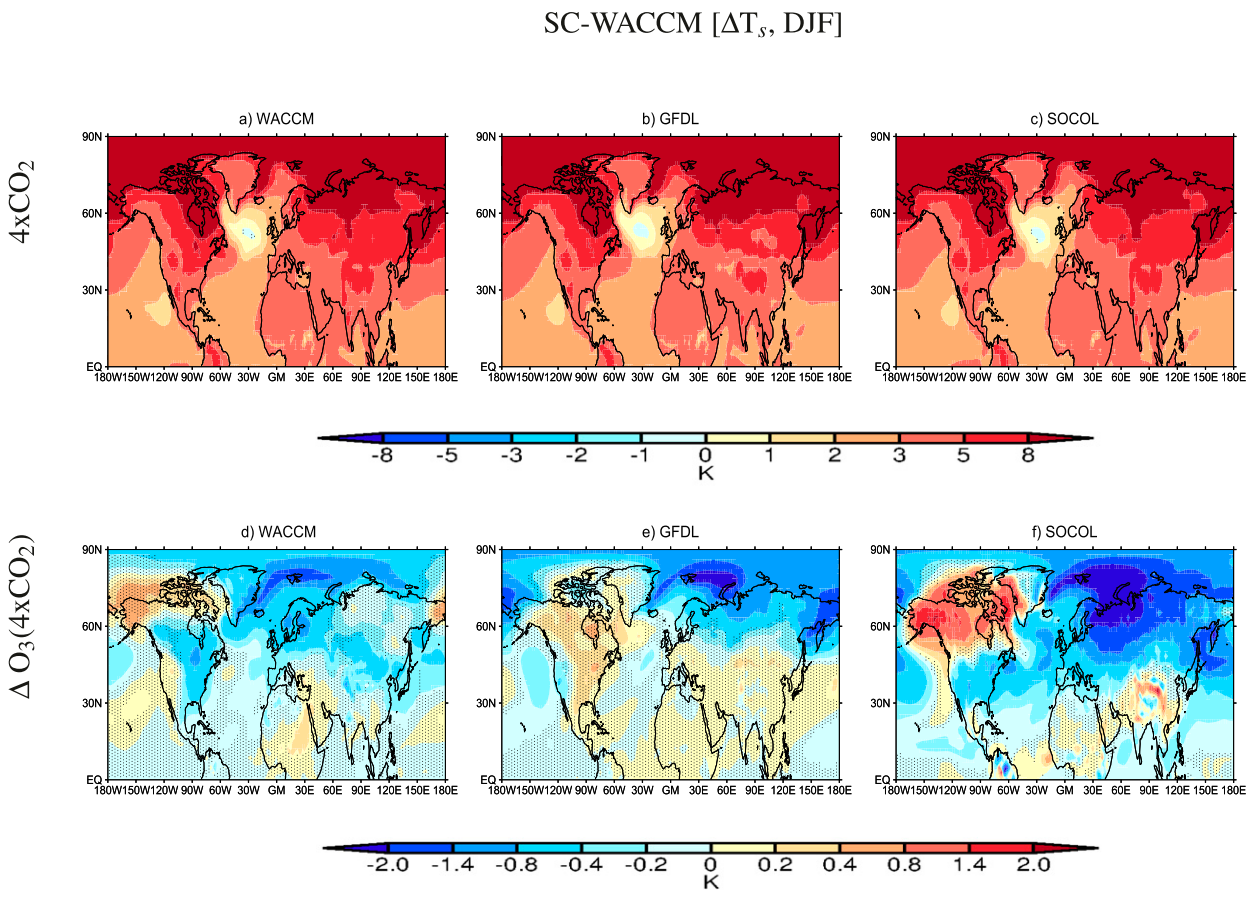

FIG. 7. (a)–(c) Boreal winter (DJF) mean surface temperature response to $4 \times CO_2$ in SC-WACCM integrations imposing the piControl ozone climatology from the (a) WACCM, (b) GFDL, and (c) SOCOL model. (d)–(f) Change in surface temperature in SC-WACCM, induced by $\Delta O_3(4 \times CO_2)$ in (d) WACCM, (e) GFDL, and (f) SOCOL. Units: K. Nonsignificant differences (at the 95% confidence level) are stippled.

climate change scenarios, to the degree that climate responses are linear to the forcing magnitude.

5. Discussion and conclusions

We have investigated the climatic implications of the ozone response to an abrupt quadrupling of CO_2, by imposing the range of ozone responses $\Delta O_3(4 \times CO_2)$ across three different coupled CCMs in one climate model, SC-WACCM. The main results are as follows:

- The pattern of $\Delta O_3(4 \times CO_2)$ produces a negligible global-mean R_{adj}. This is largely due to opposing contributions of LW and SW fluxes and cancellation between negative and positive R_{adj} in low and high latitudes.
- Consistent with the small global-mean R_{adj}, $\Delta O_3(4 \times CO_2)$ does not impact the climate sensitivity of SC-WACCM. This also holds for ozone datasets derived from CCMs showing a large negative tropical R_{adj}, such as SOCOL.
- In spite of its small impact on global-mean surface temperature, $\Delta O_3(4 \times CO_2)$ considerably affects stratospheric temperatures, reducing the meridional temperature gradient in the lower stratosphere.
- Ozone-induced stratospheric temperature changes affect the tropospheric circulation, resulting in an equatorward shift of the SH midlatitude jet in all seasons, which opposes the (CO_2 induced) poleward shift.
- In boreal winter, $\Delta O_3(4 \times CO_2)$ also substantially affects the circulation in the NH, resulting in changes to Eurasian surface climate, such as cooling and drying over northern Europe. These effects generally oppose those caused by increased CO_2 levels and are robust across the three different ozone forcing datasets used in this study.

In this paper, we have imposed the ozone response to CO_2 as a ''forcing'' in climate sensitivity experiments.

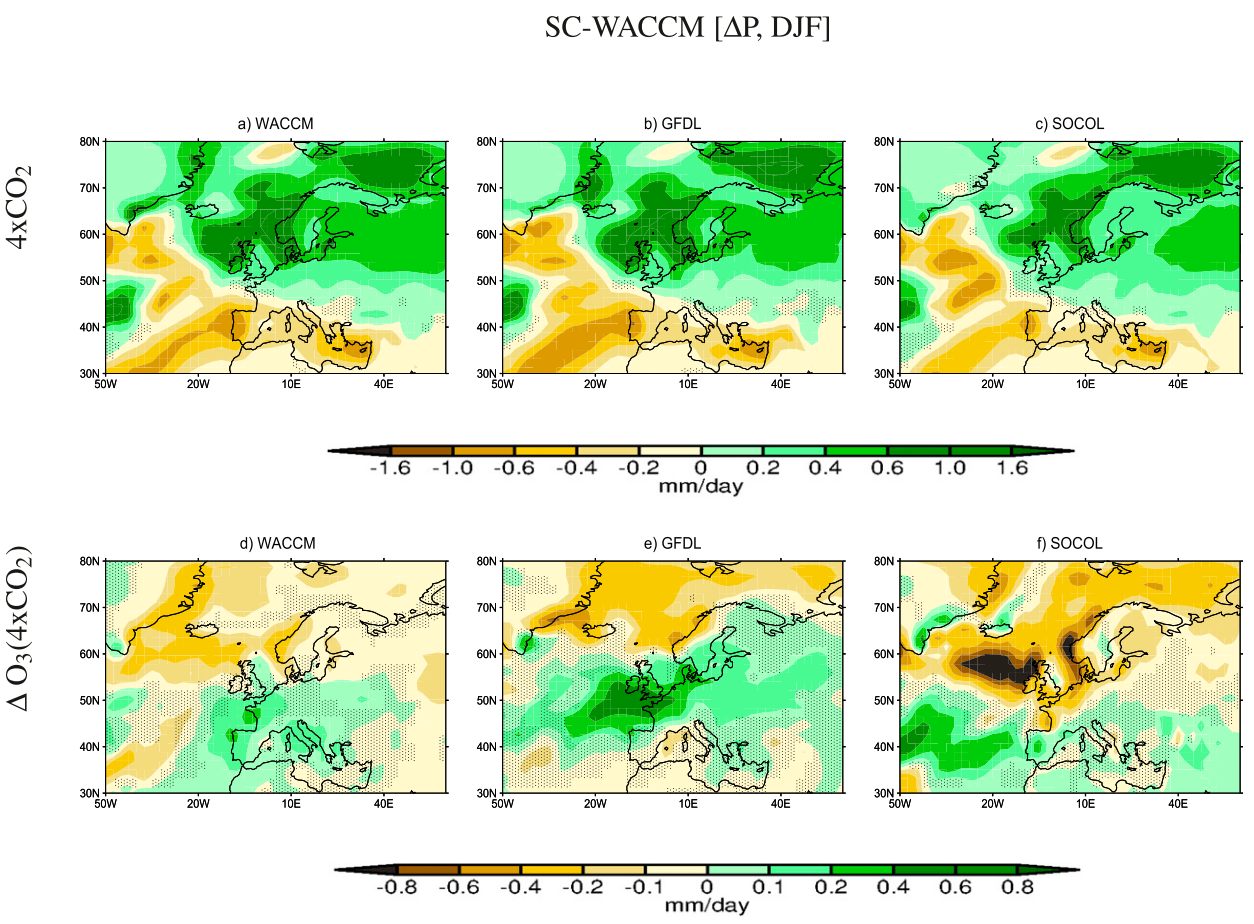

FIG. 8. (a)–(c) Boreal winter (DJF) mean precipitation response to 4 × CO_2 over the North Atlantic and Eurasia in SC-WACCM integrations imposing the piControl ozone climatology from (a) WACCM, (b) GFDL, and (c) SOCOL. (d)–(f) Change in precipitation in SC-WACCM, induced by $\Delta O_3(4 \times CO_2)$ in (d) WACCM, (e) GFDL, and (f) SOCOL. Units: mm day^{-1}. Nonsignificant differences (at the 95% confidence level) are stippled.

As shown in previous studies (Nowack et al. 2015, 2018), this "semi-offline" approach is useful to reproduce the behavior of a chemistry climate model using a model without interactive ozone chemistry. One may, however, question the validity of this approach. That is, does SC-WACCM reproduce the response to 4 × CO_2 simulated by the model configuration with interactive ozone chemistry (WACCM)? To answer this, we compared the 4 × CO_2 integration from SC-WACCM against the WACCM integration with interactive ozone documented in Chiodo and Polvani (2017) and found that the SC-WACCM integrations with 4 × CO_2 and piControl ozone (W4x and W4xO_3) are indistinguishable from WACCM 4 × CO_2 integrations, both in global-mean temperature, as shown in Marsh et al. (2016), and also in their simulated circulation response (not shown). Hence, in agreement with Nowack et al. (2015, 2018), prescribing the ozone as a forcing in a model without interactive chemistry, as we do in this paper, is a valid approach to reproduce the climate of a CCM, and thus any changes induced by the ozone response to 4 × CO_2.

Confirming earlier studies based on this same model (Marsh et al. 2016; Chiodo and Polvani 2017), we find that ozone, as it responds to 4 × CO_2, does not reduce the projected global-mean surface temperature increase. This also holds for ozone forcings exhibiting larger changes in the TLS, such as SOCOL. Due to large cancellation between R_{adj} at high and low latitudes, ozone is unlikely to induce a sizable effect on global-mean temperature projections. Hence, uncertainty in the ozone response is unlikely to explain model dependencies in the ozone feedback documented in earlier studies (Dietmüller et al. 2014; Nowack et al. 2015; Marsh et al. 2016).

The caveat here is that our results are based on a single model (SC-WACCM). This model, like its interactive chemistry counterpart (WACCM) may not be realistically sensitive to negative feedbacks induced by ozone, for example, due to missing (or weaker)

interaction between ozone and other physical feedbacks, such as clouds and/or lapse rate. The next step, we suggest, is to study the impact of the *same* ozone forcing in *different* climate models. Also, the effects of zonal asymmetries of ozone on the circulation needs to be carefully quantified; this will be of special interest for the SH, given the larger asymmetries there in the modeled ozone response in 4 × CO_2 (cf. C18, their Fig. 10) and also the presence of large depletion and recovery trends (Crook et al. 2008; Waugh et al. 2009). These issues will be investigated in a follow-up study.

In spite of these caveats, our results demonstrate that the ozone layer can significantly reduce the dynamical sensitivity, quantified in terms of the poleward shift of the midlatitude jet in response to anthropogenic greenhouse gases (e.g., Grise and Polvani 2014a). Therefore, it is important to produce CO_2-consistent ozone forcing datasets for models without interactive chemistry, as suggested by Eyring et al. (2013). Moreover, it would also be desirable to include the CCM-related uncertainty in projected CO_2-induced changes in the ozone layer.

Acknowledgments. This work is funded, in part, by a grant from the U.S. National Science Foundation to Columbia University. G.C. is also funded by a cooperative agreement between NASA and Columbia University, and by the SNF Ambizione Grant PZ00P2-180043. The model data can be made available by request to G.C.

REFERENCES

Baldwin, M. P., and T. J. Dunkerton, 2001: Stratospheric harbingers of anomalous weather regimes. *Science*, **294**, 581–584, https://doi.org/10.1126/science.1063315.

Barnes, E. A., and L. Polvani, 2013: Response of the midlatitude jets, and of their variability, to increased greenhouse gases in the CMIP5 models. *J. Climate*, **26**, 7117–7135, https://doi.org/10.1175/JCLI-D-12-00536.1.

Calvo, N., L. M. Polvani, and S. Solomon, 2015: On the surface impact of Arctic stratospheric ozone extremes. *Environ. Res. Lett.*, **10**, 094003, https://doi.org/10.1088/1748-9326/10/9/094003.

Charlton, A. J., and L. M. Polvani, 2007: A new look at stratospheric sudden warmings. Part I: Climatology and modeling benchmarks. *J. Climate*, **20**, 449–469, https://doi.org/10.1175/JCLI3996.1.

Chiodo, G., and L. M. Polvani, 2017: Reduced Southern Hemispheric circulation response to quadrupled CO_2 due to stratospheric ozone feedback. *Geophys. Res. Lett.*, **44**, 465–474, https://doi.org/10.1002/2016GL071011.

——, L. Polvani, D. Marsh, A. Stenke, W. Ball, E. Rozanov, S. Muthers, and K. Tsigaridis, 2018: The response of the ozone layer to quadrupled CO_2 concentrations. *J. Climate*, **31**, 3893–3907, https://doi.org/10.1175/JCLI-D-17-0492.1.

Collins, M., and Coauthors, 2013: Long-term climate change: Projections, commitments and irreversibility. *Climate Change 2013: The Physical Science Basis*, T. F. Stocker et al., Eds., Cambridge University Press, 1029–1136.

Conley, A., J. Lamarque, F. Vitt, W. Collins, and J. Kiehl, 2013: PORT, a CESM tool for the diagnosis of radiative forcing. *Geosci. Model Dev.*, **6**, 469–476, https://doi.org/10.5194/gmd-6-469-2013.

Crook, J. A., N. P. Gillett, and S. P. Keeley, 2008: Sensitivity of Southern Hemisphere climate to zonal asymmetry in ozone. *Geophys. Res. Lett.*, **35**, L07806, https://doi.org/10.1029/2007GL032698.

Dietmüller, S., M. Ponater, and R. Sausen, 2014: Interactive ozone induces a negative feedback in CO_2-driven climate change simulations. *J. Geophys. Res. Atmos.*, **119**, 1796–1805, https://doi.org/10.1002/2013JD020575.

Donner, L. J., and Coauthors, 2011: The dynamical core, physical parameterizations, and basic simulation characteristics of the atmospheric component AM3 of the GFDL global coupled model CM3. *J. Climate*, **24**, 3484–3519, https://doi.org/10.1175/2011JCLI3955.1.

Douglass, A., S. Strahan, L. Oman, and R. Stolarski, 2014: Understanding differences in chemistry climate model projections of stratospheric ozone. *J. Geophys. Res. Atmos.*, **119**, 4922–4939, https://doi.org/10.1002/2013JD021159.

Eyring, V., and Coauthors, 2013: Long-term ozone changes and associated climate impacts in CMIP5 simulations. *J. Geophys. Res. Atmos.*, **118**, 5029–5060, https://doi.org/10.1002/JGRD.50316.

——, S. Bony, G. A. Meehl, C. A. Senior, B. Stevens, R. J. Stouffer, and K. E. Taylor, 2016: Overview of the Coupled Model Intercomparison Project phase 6 (CMIP6) experimental design and organization. *Geosci. Model Dev.*, **9**, 1937–1958, https://doi.org/10.5194/gmd-9-1937-2016.

Goody, R. M., and Y. L. Yung, 1989: *Atmospheric Radiation: Theoretical Basis*. 2nd ed. Oxford University Press, 544 pp.

Grise, K. M., and L. M. Polvani, 2014a: Is climate sensitivity related to dynamical sensitivity? A Southern Hemisphere perspective. *Geophys. Res. Lett.*, **41**, 534–540, https://doi.org/10.1002/2013GL058466.

——, and ——, 2014b: The response of midlatitude jets to increased CO_2: Distinguishing the roles of sea surface temperature and direct radiative forcing. *Geophys. Res. Lett.*, **41**, 6863–6871, https://doi.org/10.1002/2014GL061638.

——, and ——, 2016: Is climate sensitivity related to dynamical sensitivity? *J. Geophys. Res.*, **121**, 5159–5176, https://doi.org/10.1002/2015JD024687.

Haigh, J., and J. Pyle, 1982: Ozone perturbation experiments in a two-dimensional circulation model. *Quart. J. Roy. Meteor. Soc.*, **108**, 551–574, https://doi.org/10.1002/qj.49710845705.

Hansen, J., and Coauthors, 2005: Efficacy of climate forcings. *J. Geophys. Res.*, **110**, D18104, https://doi.org/10.1029/2005JD005776.

Hurrell, J. W., Y. Kushnir, G. Ottersen, and M. Visbeck, 2003: An overview of the North Atlantic oscillation. *The North Atlantic Oscillation: Climatic Significance and Environmental Impact*, *Geophys. Monogr.*, Vol. 134, Amer. Geophys. Union, 1–35, https://doi.org/10.1029/134GM01.

Isaksen, I. S., and Coauthors, 2009: Atmospheric composition change: Climate-chemistry interactions. *Atmos. Environ.*, **43**, 5138–5192, https://doi.org/10.1016/j.atmosenv.2009.08.003.

Ivy, D. J., S. Solomon, N. Calvo, and D. W. Thompson, 2017: Observed connections of Arctic stratospheric ozone extremes to Northern Hemisphere surface climate. *Environ. Res. Lett.*, **12**, 024004, https://doi.org/10.1088/1748-9326/AA57A4.

Jonsson, A., J. De Grandpre, V. Fomichev, J. McConnell, and S. Beagley, 2004: Doubled CO_2-induced cooling in the middle atmosphere: Photochemical analysis of the ozone radiative

feedback. *J. Geophys. Res. Lett.*, **109**, D24103, https://doi.org/10.1029/2004JD005093.

Joshi, M., K. Shine, M. Ponater, N. Stuber, R. Sausen, and L. Li, 2003: A comparison of climate response to different radiative forcings in three general circulation models: Towards an improved metric of climate change. *Climate Dyn.*, **20**, 843–854, https://doi.org/10.1007/s00382-003-0305-9.

Knutti, R., and G. C. Hegerl, 2008: The equilibrium sensitivity of the Earth's temperature to radiation changes. *Nat. Geosci.*, **1**, 735–743, https://doi.org/10.1038/ngeo337.

——, M. A. Rugenstein, and G. C. Hegerl, 2017: Beyond equilibrium climate sensitivity. *Nat. Geosci.*, **10**, 727–736, https://doi.org/10.1038/ngeo3017.

Lacis, A. A., D. J. Wuebbles, and J. A. Logan, 1990: Radiative forcing of climate by changes in the vertical distribution of ozone. *J. Geophys. Res.*, **95**, 9971–9981, https://doi.org/10.1029/JD095iD07p09971.

Lin, P., D. Paynter, L. Polvani, G. J. Correa, Y. Ming, and V. Ramaswamy, 2017: Dependence of model-simulated response to ozone depletion on stratospheric polar vortex climatology. *Geophys. Res. Lett.*, **44**, 6391–6398, https://doi.org/10.1002/2017GL073862.

Marsh, D. R., M. J. Mills, D. E. Kinnison, J.-F. Lamarque, N. Calvo, and L. M. Polvani, 2013: Climate change from 1850 to 2005 simulated in CESM1 (WACCM). *J. Climate*, **26**, 7372–7391, https://doi.org/10.1175/JCLI-D-12-00558.1.

——, J.-F. Lamarque, A. J. Conley, and L. M. Polvani, 2016: Stratospheric ozone chemistry feedbacks are not critical for the determination of climate sensitivity in CESM1 (WACCM). *Geophys. Res. Lett.*, **43**, 3928–3934, https://doi.org/10.1002/2016GL068344.

Maycock, A., 2016: The contribution of ozone to future stratospheric temperature trends. *Geophys. Res. Lett.*, **43**, 4609–4616, https://doi.org/10.1002/2016GL068511.

Miller, R. L., and Coauthors, 2014: CMIP5 historical simulations (1850–2012) with GISS ModelE2. *J. Adv. Model. Earth Syst.*, **6**, 441–477, https://doi.org/10.1002/2013MS000266.

Muthers, S., and Coauthors, 2014: The coupled atmosphere–chemistry–ocean model SOCOL-MPIOM. *Geosci. Model Dev.*, **7**, 2157–2179, https://doi.org/10.5194/gmd-7-2157-2014.

Myhre, G., and Coauthors, 2013: Anthropogenic and natural radiative forcing. *Climate Change 2013: The Physical Science Basis*, T. Stocker et al., Eds., Cambridge University Press, 659–740.

Neely, R., D. Marsh, K. Smith, S. Davis, and L. Polvani, 2014: Biases in Southern Hemisphere climate trends induced by coarsely specifying the temporal resolution of stratospheric ozone. *Geophys. Res. Lett.*, **41**, 8602–8610, https://doi.org/10.1002/2014GL061627.

Nowack, P. J., N. L. Abraham, A. C. Maycock, P. Braesicke, J. M. Gregory, M. M. Joshi, A. Osprey, and J. A. Pyle, 2015: A large ozone-circulation feedback and its implications for global warming assessments. *Nat. Climate Change*, **5**, 41–45, https://doi.org/10.1038/NCLIMATE2451.

——, P. Braesicke, N. L. Abraham, and J. A. Pyle, 2017: On the role of ozone feedback in the ENSO amplitude response under global warming. *Geophys. Res. Lett.*, **44**, 3858–3866, https://doi.org/10.1002/2016GL072418.

——, N. L. Abraham, P. Braesicke, and J. A. Pyle, 2018: The impact of stratospheric ozone feedbacks on climate sensitivity estimates. *J. Geophys. Res.*, **123**, 4630–4641, https://doi.org/10.1002/2017JD027943.

Oman, L., and Coauthors, 2010: Multimodel assessment of the factors driving stratospheric ozone evolution over the 21st century. *J. Geophys. Res.*, **115**, D24306, https://doi.org/10.1029/2010JD014362.

Ramanathan, V., and R. E. Dickinson, 1979: The role of stratospheric ozone in the zonal and seasonal radiative energy balance of the earth-troposphere system. *J. Atmos. Sci.*, **36**, 1084–1104, https://doi.org/10.1175/1520-0469(1979)036<1084:TROSOI>2.0.CO;2.

Seviour, W. J., A. Gnanadesikan, and D. W. Waugh, 2016: The transient response of the Southern Ocean to stratospheric ozone depletion. *J. Climate*, **29**, 7383–7396, https://doi.org/10.1175/JCLI-D-16-0198.1.

Shepherd, T. G., 2008: Dynamics, stratospheric ozone, and climate change. *Atmos.–Ocean*, **46**, 117–138, https://doi.org/10.3137/ao.460106.

——, 2014: Atmospheric circulation as a source of uncertainty in climate change projections. *Nat. Geosci.*, **7**, 703–708, https://doi.org/10.1038/ngeo2253.

Smith, K. L., and L. M. Polvani, 2014: The surface impacts of Arctic stratospheric ozone anomalies. *Environ. Res. Lett.*, **9**, 074015, https://doi.org/10.1088/1748-9326/9/7/074015.

——, R. Neely, D. Marsh, and L. Polvani, 2014: The Specified Chemistry Whole Atmosphere Community Climate Model (SC-WACCM). *J. Adv. Model. Earth Syst.*, **6**, 883–901, https://doi.org/10.1002/2014MS000346.

Stenke, A., M. Schraner, E. Rozanov, T. Egorova, B. Luo, and T. Peter, 2013: The SOCOL version 3.0 chemistry–climate model: Description, evaluation, and implications from an advanced transport algorithm. *Geosci. Model Dev.*, **6**, 1407–1427, https://doi.org/10.5194/gmd-6-1407-2013.

Stuber, N., M. Ponater, and R. Sausen, 2001: Is the climate sensitivity to ozone perturbations enhanced by stratospheric water vapor feedback? *Geophys. Res. Lett.*, **28**, 2887–2890, https://doi.org/10.1029/2001GL013000.

——, ——, and ——, 2005: Why radiative forcing might fail as a predictor of climate change. *Climate Dyn.*, **24**, 497–510, https://doi.org/10.1007/s00382-004-0497-7.

Waugh, D., L. Oman, P. Newman, R. Stolarski, S. Pawson, J. Nielsen, and J. Perlwitz, 2009: Effect of zonal asymmetries in stratospheric ozone on simulated Southern Hemisphere climate trends. *Geophys. Res. Lett.*, **36**, L18701, https://doi.org/10.1029/2009GL040419.

WMO, 2014: Scientific Assessment of Ozone Depletion: 2014. World Meteorological Organization Rep. 55, https://www.wmo.int/pages/prog/arep/gaw/ozone_2014/documents/Full_report_2014_Ozone_Assessment.pdf.

Zubov, V., E. Rozanov, T. Egorova, I. Karol, and W. Schmutz, 2013: Role of external factors in the evolution of the ozone layer and stratospheric circulation in 21st century. *Atmos. Chem. Phys.*, **13**, 4697–4706, https://doi.org/10.5194/acp-13-4697-2013.